

Localization of Reflection Induced Multi-Path-Interference Over Multi-Span Transmission Link by Receiver-side Digital Signal Processing

Choloong Hahn⁽¹⁾, Junho Chang⁽¹⁾, Zhiping Jiang^{(1)*}

⁽¹⁾Huawei Technologies Canada, 303 Terry Fox Drive, Ottawa, Canada
zhiping.jiang@huawei.com

Abstract: We propose and experimentally demonstrate a localization method of reflection induced multi-path-interference over multi-span transmission link by post digital signal processing of received signal obtained by a coherent receiver at the end of the transmission. © 2021 The Author(s)

1. Introduction

Reflection induced multi-path interference (MPI) caused by a reflected signal generated by a main signal. The reflections can be generated by two consecutive Rayleigh back-scatterings in the fiber, or combinations of multiple reflections of the transmitted main signal originating from optical interfaces such as fiber connectors, transmitters, and receivers [1]. This impairment can be generated anywhere in a transmission link, and detecting the root cause and/or localization is extremely hard and time consuming, however, there is no effective way to detect and localize the MPI. Therefore, it is required to detect and especially localize the MPI in the given transmission link to effectively resolve the failure in the data transmission.

Recently, optical system monitoring and analysis methods to leverage the potential of digital coherent receiver has been proposed and investigated. By employing advanced digital signal processing and/or machine learning techniques designed for monitoring, they successfully detect and localize the local optical power [2], identify the fiber types in a link [3], and localize optical filter misalignments [4] with only the optical signals received at the receiver-end. In this paper we propose and experimentally demonstrate a MPI localization method over six spans of 75-km SSMF link with 34 GBaud DP-QPSK signal, based on the digital signal processing technique with received signal at a coherent receiver by utilizing the uniqueness of the nonlinear distortion of MPI signal. This is the first experimental confirmation of the MPI localization which requires only the received.

2. Operation principle of MPI localization

The basic principal of the MPI localization is a correlation between received total nonlinear distortions (NLD) due to the self-phase modulation (SPM) and MPI templates generated for different locations along the transmission link. From the non-commutable relation between linear and nonlinear operators, it is possible to retrieve local system parameters [2].

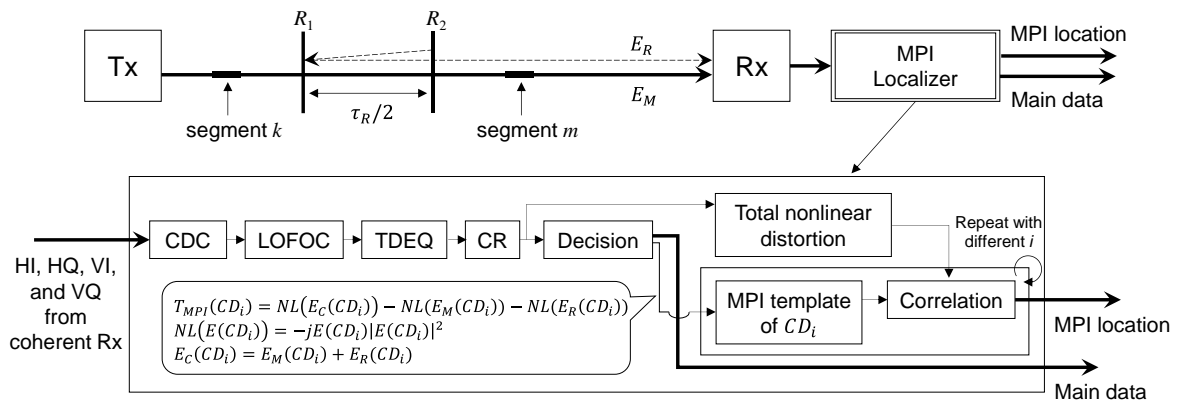


Fig. 1. Schematic diagram of an optical transmission link containing reflection induced MPI and block diagram of proposed multi-path interference localizer. Solid arrow shows main signal (E_M) propagation while dashed arrow shows reflected signal (E_R) reflected at R_2 then R_1 . CDC: chromatic dispersion compensator, LOFOC: local oscillator frequency offset compensator, TDEQ: time-domain equalizer, CR: carrier recovery

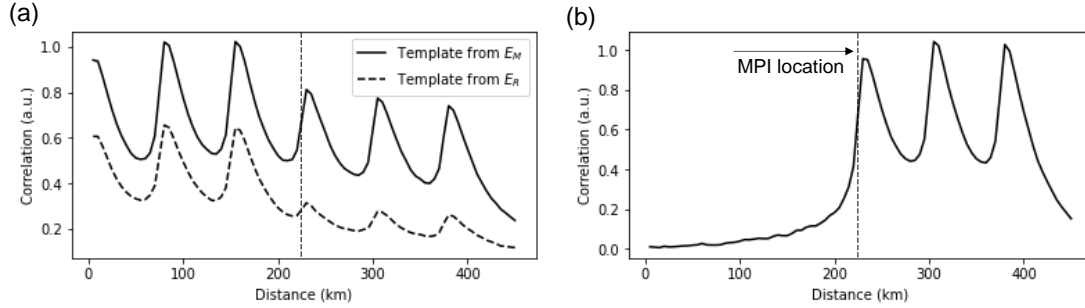


Fig. 2. Correlation between simulated total nonlinear distortions at the receiver and templates. (a) Correlation with templates generated from only E_M or E_R . (b) Templates generated from mixed E_M and E_R .

Fig. 1 is a schematic illustration of a transmission link that shows the reflection induced MPI in the middle of the propagation link. Assuming $E_M(t, CD_i)$ is the main signal transmitted from Tx and propagates to the location i of the link with accumulated chromatic dispersion CD_i . The main signal can be reflected to the backward direction at R_2 and then reflected again at R_1 which propagates again to the forward direction, therefore, it generates MPI after the R_1 with the reflected signal $E_R(t, CD_i) = \sqrt{R_t}E_M(t + \tau_R, CD_i)$, where $R_t = R_1R_2$ is the total power reflectance.

Each location along the transmission link have point-wise NLD induced by the Kerr effect based on an equation of $E(t) \exp(-j|E(t)|^2)$. For example, at segment k in Fig. 1, it becomes $E_M(t, CD_k) \exp(-jA_k|E_M(t, CD_k)|^2)$ where, CD_k is accumulated chromatic dispersion during the propagation to the location k , and A_k is the constant including the signal power and nonlinear coefficient. It can be rewritten as $E_M(t, CD_k) + NL(E_M(t, CD_k))$ when the NLD is small. This is sum of linear signal and additive NLD which can be written as below.

$$NL(E_M(t, CD_k)) = -jE_M(t, CD_k)|E_M(t, CD_k)|^2. \quad (1)$$

Since the point-wise NLD is unique due to the non-commutative relationship between the chromatic dispersion and the nonlinear operator over the transmission, the NLD generated at each location is detectable at the receiver-end by taking correlation between the received total NLD with appropriate template that can be generated from the linear signal obtained after decision by using Eq. (1).

In Fig. 2(a), the solid curve is the correlation between the received NLD and the templates generated from only E_M while the dashed curve is the correlation with templates generated from only E_R . Here the received NLD is simulated by split step method by solving nonlinear Schrödinger equation for 6×75 km SSMF transmission with 34-Gbaud, DP-QPSK signal, with 0 dBm launch power at each span input. In this simulation, the MPI generated at the 4th span which is marked as vertical dashed line in Fig. 2. The correlation curves show multiple peaks related the power change within the spans and the peak drops after the MPI location due to the longitudinal power profile of main or the reflected signal. The E_R is not existing before MPI location but the correlation with the template from E_R also shows peaks at the spans before MPI generation. This is because the NLD before MPI location also experiences the reflections at R_1 and R_2 . Thus, these correlations have peaks for all the spans before and after the reflection, but the peak values decrease after the reflection. This behaviour might be used to MPI localization, however these are not a sufficient method to localize the MPI location because the power at the spans are not typically a known parameter at the receiver side.

At the locations after the reflection, for example the segment m showed in Fig. 1, the NLD is generated from the combined signal $E_C(t, CD_m) = E_M(t, CD_m) + E_R(t, CD_m)$ with Eq. (1) which can be written as below.

$$NL(E_C) = NL(E_M) + NL(E_R) + CS, \quad (2)$$

where, CS is additional terms generated by the combination of signals E_M and E_R . Unlike the $NL(E_R)$, the CS in Eq. (2) is existing only when there exist both reflected and main signals. Therefore, the MPI location is clearly detectable by tracking the CS of the NLD by generating the template for the CS as $T_{MPI} = NL(E_C) - NL(E_M) - NL(E_R)$. Fig. 2(b) shows the correlation with T_{MPI} which has correlations after the MPI and no correlations before the MPI which implies successful detection of the MPI location.

3. Experimental results and discussion

We implemented and demonstrated the proposed MPI localization method in a dispersion-unmanaged transmission link consisting with six 75-km long SSMF spans as shown in Fig. 3(a). 34-Gbaud Nyquist-filtered DP-QPSK signal was launched at Tx with 4 dBm of power at each span.

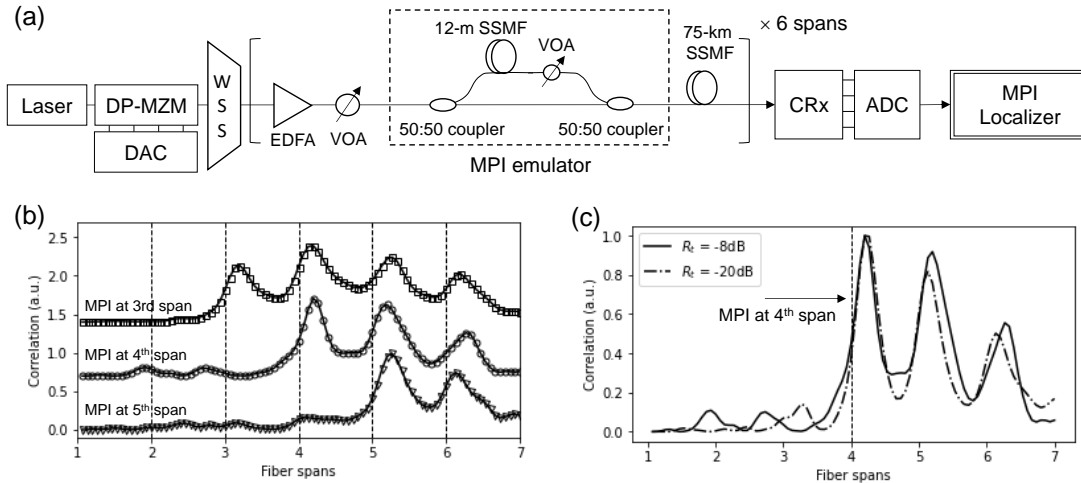


Fig. 3. (a) Experimental setup of MPI propagation and localization. DP-MZM: dual polarization Mach-Zehnder modulator, DAC digital to analog converter, WSS: wavelength selective switch, EDFA: Erbium-doped fiber amplifier, VOA: variable optical attenuator, SSMF: standard single-mode fiber, CRx: coherent receiver, ADC: analog to digital converter. (b) MPI localization of measured signal with different MPI location. (c) MPI localization of different MPI reflectance. Vertical dashed line indicate the MPI location in the transmission link.

To mimic local reflections and resultant MPI, the signal was split into two arms with a 50:50 coupler for main and reflected signal transmission. In the reflected signal arm, an extra 12-m long SSMF and an optical attenuator were added to emulate the MPI delay and the reflectance, respectively. The two split arms were combined again after each propagation and then launched into the rest of the transmission link. The MPI was applied at the beginning of either 3rd, 4th or 5th span. At receiver side, the signal was received and sampled by an integrated coherent receiver and a real-time sampling oscilloscope, and fed into the core part of MPI localizer as shown in Fig. 1.

The MPI localizations of measured signal which was performed with T_{MPI} are shown in Fig. 3(b) and 3(c) for different MPI conditions. Fig. 3(b) shows MPI localization of signals with different MPI location as labelled in the left-side of the figure. The measured MPI localization shows the correlation peaks appearing after the MPI location and no correlations before the MPI location. Therefore, one can clearly recognize the location of MPI reflection from the resulted correlation shown in the figure. The resulting correlation curves have oscillations after MPI location which shows longitudinal power profile due to A_k retrieved by the correlation taken between the received NLD and the templates. Thus, the oscillation also implies successful localization of MPI.

Fig. 3(c) shows MPI localization with the MPI generated at 4th span with different R_t . The solid line and dashed-dot line are the MPI localization for signals with $R_t = -8\text{ dB}$ and -20 dB , respectively. Both curves are divided by their maximum value to clearly see the MPI localization at $R_t = -20\text{ dB}$.

4. Conclusions

We proposed a digital data processing based method to localize reflection induced MPI for multi-span optical transmission link by utilizing NLD accumulated and received at a coherent receiver. The proposed correlation template for MPI localization is basically the NLD generated by combined main and reflected signals, which can only exist where there is MPI. With the proposed MPI template, the MPI localization is experimentally demonstrated over 6 spans of 75-km SSMF transmission link with 34 GBaud DP-QPSK signal. This enables effective localization of MPI and expand the functionalities of optical system monitoring based on digital data processing.

5. References

- [1] C. R. S. Fludger, M. Mazzini, T. Kupfer, and M. Traverso, "Experimental measurements of the impact of multi-path interference on PAM signals," Optical Fiber Communication Conference (OFC) 2014, paper W1F.6, 2014.
- [2] T. Tanimura et al., "Fiber-longitudinal anomaly position identification over multi-span transmission link out of receiver-end signals," J. Lightwave Technol. vol. 38, no. 9, pp. 2726–2733, 2020.
- [3] T. Sasai et al., "Simultaneous detection of anomaly points and fiber types in multi-span transmission link only by receiver-side digital signal processing," Optical Fiber Communication Conference (OFC) 2020, paper Th1F.1, 2020
- [4] T. Sasai et al., "Digital Backpropagation for Optical Path Monitoring: Loss Profile and Passband Narrowing Estimation," 2020 European Conference on Optical Communications (ECOC), 2020, pp. 1-4, doi: 10.1109/ECOC48923.2020.9333191, 2020.